THINK INDIA JOURNAL

ISSN:0971-1260
Vol-22-Issue-37-December -2019

Detailed Investigation of Modelling Characteristics for LPFG using Triple Layer Geometry

[1]Jai Sukh Paul Singh, [2]Paramvir Singh
[1]*Division of Research and Development,* [2]*School of Electronics and Communiation*
[1,2]*Lovely Professional University*
Phagwara, Punjab, India.

[1]khalsa128@gmail.com
[2]paramvir240.singh@gmail.com

Abstract

In this research paper, performance analysis of different modelling characteristics using Long Period Fiber Grating (LPFG) is performed. Different parameters such as cladding effective index, core effective index, coupled mode theory, coupling coefficient and transmission spectrum of Long period Fiber grating are calculated and analyzed. The Proposed modeling aspects based on Triple layer geometry is compared with the existing double layer modelling of LPFG. The double layer geometry is very simple, but suffers from the weakly guided approximation whereas this triple layer geometry is very complicated and problematic but very accurate results are obtained for hypothetical understanding of Long Period Fiber Grating. All the results obtained are simulated using MATLAB.

Keywords—Triple Layer Geometry,Three layer geometry, Two layer geometry, Long Period Fiber Grating, Coupling coefficient, Formula method, Transmission Spectrum, Integral method, Transmission matrix method

I. INTRODUCTION

In optical communication and sensing systems, optical devices like Long period Fiber Grating (LPFG) are found to possess various applications. Fiber gratings are designed by crafting a part of periodically varied refractive index among the core of associate optical fiber. Fiber gratings are classified as Fiber Bragg Grating (FBG) or LPFG based mostly upon the grating amount. LPFG's have grating period within the vary of one hundred micros to one millimeter whereas FBG's have sub-micro period. *Vengsarkar et. al.* [1] in 1995 developed a LPFG as a band rejection optical filter. during this LPFG stimulates the coupling between the assorted propagation modes as LP_{01} mode accessible within the core and LP0m (where m = 1, 2, 3, …) because the co-propagation facing modes within the rattled region as delineated within the Fig. 1. Therefore, the transmission spectrum that is created, include series of attenuation bands at varied separate resonant wavelengths.

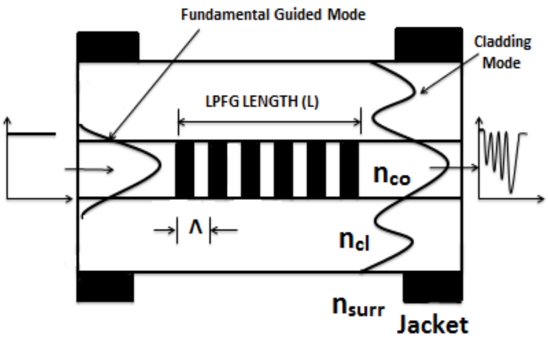

Fig. 1. Coupling of primary guided mode to cladding mode in LPFG.

The equation and condition used to match phase between the fundamental guided core more and other different forward co-propagation cladding modes in LPFG is illustrated as under [1].

$$\lambda_{res} = \left(n_{eff,co}(\lambda) - n^{m}_{eff,cl}(\lambda)\right)\Lambda \qquad (1)$$

In this resonant wavelength is represented as λ_{res}, and effective refractive index is denoted as $n_{eff,co}$, where as $n^{m}_{eff,cl}$ is the effective refractive index of m^{th} cladding mode. The grating period of the fiber is denoted as 'Λ'.

As an application point of view LPFG devices are used for various purposes in optical communication systems such as band stop filters [1], refractive index sensors [3] and temperature and strain sensors [2]. The sensors designed using this LPFG have numerous advantages over the traditional conventional sensors. Even these sensors are very light and relatively small in size as compared to other sensors, still they have very good sensitivity, free from corrosion attack [4] and electromagnetic interferences [5] but at the same time great long-term stability[6].

In the most straightforward terms, the recreation technique happens as pursues. Initially the propagation constant of theessential core and cladding modes are determined to decide the viable refractive indices of the core and cladding modes. Secondly, at that point the coupling coefficient is obtained for coupling between explicit modes.Lastly the total transmission range is analyzed utilizing coupled-mode hypothesis.

II. Double layer geometry and Triple Layer Geometry

Going through an intense literature shows that there are two distinctive methodologies exist for hypothetically displaying of LPFG transmission spectrum. the primary methodology is planned by *Vengsarkar et. al.* [1], who delineated the new development of LPFG and the second, planned by *Erdogan et. al.* [7], uncovered the inaccuracies and deficiencies of the first technique. They consequently giving a invigorated, actual strategy nevertheless brings concerning extraordinary numerical complexness. The principle distinction between these two methodologies lies in their portrayal of the fiber pure mathematics, that is finally depended upon to see separate articulations for the scattering relations, mode field profiles, and coupling coefficients. whereas the two ways utilize the weakly guided approximation to find the effective refractive index of the basic core mode. both the higher than mentioned methodologies contradict in terms of the way by that the cladding effective mode index are determined [7]. In this paper the weakly guided approximation is taken into account as low Δ fibers [7], in which: -

$$\Delta = \frac{n_{co}-n_{cl}}{n_{co}} \ll 1 \qquad (2)$$

'Δ' is referred as the normalized core-cladding index difference. the above presumption permits easier arrangement of the trademark conditions, which approximates the accurate solutions [9]. Though, *Erdogan et. al.* [7] utilizes three-layer geometry having definite vector-field portrayals for the figuring of cladding modes. In this technique, the impact of the center is being fused when figuring the effective modalindex of the cladding. There are very few research papers who discussed LPFG modelling by using three-layer geometry because this technique has higher complexity, but in this paper, efforts have been made to explain step by step the complete description of how three-layer geometry is used for theoretically modelling of LPFG to get better results. This paper islimited to those equations which are helpful and used for modelling of LPFG in triple layer geometry to save excessive mathematical complexity.

III. Numerical Analysis for Core Effective Index

The core mode of propagation is found from Linearly Polarized mode scattering relation inthe form of an Eigen value condition. In this methodology the internal chamber is comprised of core and external chamber made up of boundless and uniform cladding [8].

$$u_{co}\left(\frac{J_1(u_{co})}{J_0(u_{co})}\right) = w_{co}\left(\frac{K_1(w_{co})}{K_0(w_{co})}\right) \qquad (3)$$

In the above equation $J_0(u_{co})$ and $J_1(u_{co})$ are the Bessel functions of the kind1st and order zero and one respectively. Whereas, $K_0(w_{co})$ and $K_1(w_{co})$ indicates the modified Bessel function of the kind 2nd and order zero and one respectively. In the above equation u_{co} and w_{co} are considered as the normalized transverse wave numbers, which can be expressed in the terms of optical fiber's V-number. The inter-relationship between w_{co} and u_{co} is expressed as follows:

$$w_{co}^2 + u_{co}^2 = V^2 \qquad (4)$$

By using the graphical method of the above mathematical expression, the intersection points and the corresponding value of u_{co} can be obtained.

$$\beta_{co} = \sqrt{(fn_{co})^2 - \left(\frac{u_{co}}{a_{co}}\right)^2} \qquad (5)$$

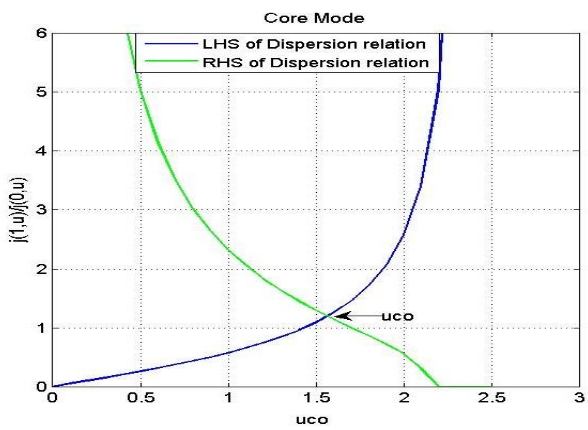

Fig. 2. Graphical representation of numerical analysis of core mode.

$$n_{eff} = \frac{\beta_{co}}{f} \qquad (6)$$

where *'b'* is the normalized effective index and is used later, and $f = \frac{2\pi}{\lambda}$. *'f'* is the free space propagation constant 'b' is further expressed as:

$$b = \frac{n_{eff}^2 - n_{cl}^2}{n_{co}^2 - n_{cl}^2} \tag{7}$$

where, $n_{cl} < n_{eff} < n_{co}$ and a_{co} is the core radius, n_{co} is thecore refractive index and n_{cl} is the cladding refractive index.

IV. Double layer geometry and Triple Layer Geometry

Utilizing two-layer geometry, weakly guided estimate that 'Δ' is extremely little, so mistakes of this strategy are rectified by utilizing triple-layer geometry. In this strategy core cladding interface isn't disregarded, and the necessary scattering connection for different cladding mode is given as follows [7]:

$$\zeta_0 = \zeta_0' \tag{8}$$

Where:

$$\zeta_0 = \frac{\frac{1}{\sigma_2}\left\{\left[JK + \left(\frac{\sigma_1\sigma_2 u_{21} u_{32}}{a_{co} a_{cl} n_{cl}^2}\right)\right] u_2 p_v(a_{cl}) - K q_v(a_{cl}) + J r_v(a_{cl}) - \frac{s_v(a_{cl})}{u_2}\right\}}{-\left[\left(\frac{u_{32}}{a_{cl} n_{cl}^2}\right) J - \left(\frac{u_{21}}{a_{co} n_{co}^2}\right) K\right] u_2 p_v(a_{cl}) + \frac{u_{32} q_v(a_{cl})}{a_{cl} n_{co}^2} + \frac{u_{21} r_v(a_{cl})}{a_{co} n_{co}^2}} \tag{9}$$

$$\zeta_0' = \frac{\sigma_1\left\{\left[\left(\frac{u_{32}}{a_{cl}}\right) J - \left(\frac{u_{21} n_{ext}^2}{a_{co} n_{cl}^2}\right) K\right] u_2 p_v(a_{cl}) - \left(\frac{u_{32} q_v(a_{cl})}{a_{cl}}\right) - \left(\frac{u_{21} r_v(a_{cl})}{a_{co}}\right)\right\}}{\left[\left(\frac{n_{surr}^2}{n_{cl}^2}\right) JK + \left(\frac{\sigma_1\sigma_2 u_{21} u_{32}}{a_{co} a_{cl} n_{co}^2}\right)\right] u_2 p_v(a_{cl}) - \left[\frac{q_v(a_{cl}) n_{surr}^2}{n_{co}^2}\right] K + J r_v(a_{cl}) - \frac{s_v(a_{cl}) n_{cl}^2}{u_2 n_{co}^2}} \tag{10}$$

Where $\sigma_1 = j\left(\frac{v n_{eff}}{Z_0}\right)$ and $\sigma_2 = j(v n_{ef} Z_0)$ and

$$u_1 = \sqrt{\left(\frac{2\pi}{\lambda}\right)^2 (n_{co}^2 - n_{eff}^2)} \tag{11}$$

$$u_2 = \sqrt{\left(\frac{2\pi}{\lambda}\right)^2 (n_{cl}^2 - n_{eff}^2)} \tag{12}$$

$$w_3 = \sqrt{\left(\frac{2\pi}{\lambda}\right)^2 (n_{eff}^2 - n_{ext}^2)} \tag{13}$$

$$u_{21} = \frac{1}{{u_2}^2} - \frac{1}{{u_1}^2} \tag{14}$$

$$u_{32} = \frac{1}{{w_3}^2} + \frac{1}{{u_2}^2} \tag{15}$$

In all of above conditions, $Z_0 = \sqrt{\mu_0/\varepsilon_0} = 377\Omega$ is the free space electromagnetic impedance *'N'* is characterized as a Bessel capacity of the second kind or the Neumann function, and the azimuthal order of the cladding mode is set to v=1 all together for non-zero coupling to happen with the circularly symmetric core mode. This methodology permits direct computation of the cladding modes effective indices of refraction by methods for deciding the crossing point focuses in the graphical portrayal of the scattering connection given in condition (8) and appeared in Fig. 3 below.

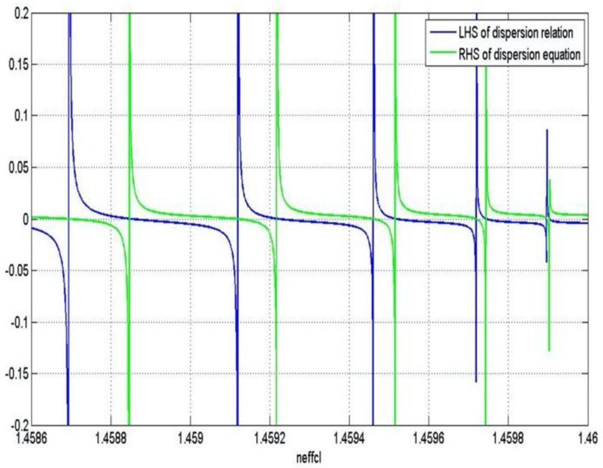

Fig. 3. Graphical representation of numerical analysis of cladding mode's effective indices using Triple-Layer geometry.

V. Coupling Coefficient of Core Mode and Different Cladding Modes

Fiber gratings are etched to border an intermittent refractive index profile within the core of an optical fiber. This causes an perturbation within the effective mode index of the chief guiding modes, given once all is claimed generally expression as bellow [10].

$$n_{co}(z) = n_{co}\left\{1 + \sigma(z)\left[1 + x\cos\left(\frac{2\pi}{\Lambda}z\right)\right]\right\} \tag{16}$$

Heren_{co} is the unperturbed core refractive index; 'Λ' is the period of the grating, 'x' is the fringevisibility of the index change, where $0 \leqslant x \leqslant 1$, and σ (z)is the gradually shifting envelope of the grating. Equation (22) can be written as:

$$n_{co}(z) = n_{co} + n_{co}\sigma(z)\left[1 + x\cos\left(\frac{2\pi}{\Lambda}z\right)\right] \tag{17}$$

This adjustment reveals that the peak induced index change at any 'z' is given as $n_{co}\ \sigma(z)[1 + x]$ when $cos({}^{2\pi}/_{\Lambda}\ z)$ is equivalent to 1 and least inducedindex change at any 'z' is given as $n_{co}\ \sigma(z)[1 - x]$ when $cos({}^{2\pi}/_{\Lambda})\ z$ is equivalent to -1. Where $n_{co}\ \sigma(z)$ depicts the profile of dc induced index change, taking average over the grating period.

In this perturbed area, core mode couple capacity to different co-propagating cladding modes LP_{0m}. Erdogan [7] utilizes careful field dispersions in LPFG displaying and in this manner coupling coefficient between core mode LP_{01} and different cladding modes LP_{0m} is given underneath [7]:

$$K_{1m-01}^{cl-co}(z) = \sigma(z)f\left(\frac{\pi b}{Z_0 n_{cl}\sqrt{1+2b\Delta}}\right)^{\frac{1}{2}} \times \frac{n_{co}^2 u_1}{u_1^2 - \frac{V^2(1-b)}{a_{co}^2}} \times \left(1 + \frac{\sigma_2\zeta_0}{n_{co}^2}\right)E_{1m}^{cl}\left[u_1 J_1(u_1 a_{co}) \times \frac{J_0 V\sqrt{1-b}}{J_1(V\sqrt{1-b})} - \frac{V\sqrt{1-b}}{a_{co}}J_0(u_1 a_{co})\right] \tag{18}$$

Peak induced index change is taken as $n_{co}\ \sigma(z) = 0.5 \times 10^{-4}$. The main obscure amount in above expression (24) is standardization constant E_{1m}^{cl}. Calculation can be performed for the standardization constant E_{1m}^{cl}, when, we decide the mode effective index by determining that every mode convey a power intensity of 1W. At the point when the vital is set equivalent to 1 W, as in Equation (25), the main obscure in the subsequent condition is the ideal standardization constant [7].

$$P = \frac{1}{2}\mathrm{Re}\int_0^{2\pi} d\emptyset \int_0^{\infty} r dr\left(E_r^{cl}H_{\emptyset}^{cl*} - H_r^{cl*}E_{\emptyset}^{cl}\right) = 1W \tag{19}$$

The integral along the radial direction can be broken into three parts, First, segment is the investigation of cladding modes vector segments in the fiber center '$r \leq a_{co}$'and cladding mode control in this district of activity is taken as P_1. Second,segment is the investigation of cladding modes vector segments in the fiber cladding area '$a_{co} \leq r \leq a_{cl}$' and cladding mode control in this locale of activity is taken as P_2. Third, segment is the investigation of cladding modes vector segments in the encompassing district '$r \geq a_{cl}$' and cladding mode power in this locale of activity is taken as P_3.

The overall power conveyed by the cladding mode is the aggregate of the forces conveyed in the center, the cladding, and the encompass area, or

$$p = p_1 + p_2 + p_3 = 1\ Watts \tag{20}$$

Where P1, P2, P3 can be determined by methods for the necessary in Equation (19) yet with the cutoff points along the radial direction replaced by those proper for the locale of interest. Th complex mathematical calculate is not considered in this paper, but the end equation for this calculation is given beneath [7].

$$P_{1,coeff} = \frac{\pi a_{co}^2 u_1^2}{4}\left\{\left[\frac{n_{eff}}{Z_0} - \frac{n_{eff} z_0 \zeta_0{}^2}{n_{co}^2} + \left(1 + \frac{n_{eff}^2}{n_{co}^2}\right)\right][im(\zeta_0)][J_2^2(u_1 a_{co}) - J_1(u_1 a_{co})J_3(u_1 a_{co})] + \left[\frac{n_{eff}}{Z_0} - \frac{n_{eff} Z_0 \zeta_0^2}{n_{co}^2} - \left(1 + \frac{n_{eff}^2}{n_{co}^2}\right) \times Im(\zeta_0)\right][J_0^2(u_1 a_{co}) - J_1^2(u_1 a_{co})]\right\} \tag{21}$$

$$P_1 = \left(E_{1m}^{cl}\right)^2 P_{1,coeff} \tag{22}$$

$$P_{2,coeff} = \frac{\pi^3 a_{co}^2 u_1^4 u_2^2 J_1^2(u_1 a_{co})}{16} \times \left\{\left(\frac{n_{eff}}{Z_0}F_2^2 - \frac{n_{eff} Z_0}{n_{cl}^2}G_2^2\right)(Q + \bar{Q}) + \frac{1}{u_2^2} \times \left(\frac{n_{eff}}{Z_0} - \frac{n_{eff} Z_0 n_{cl}^2 \zeta_0^2}{n_{co}^4}\right)(R + \bar{R}) + \left(1 + \frac{n_{eff}^2}{n_{cl}^2}\right)F_2 im(G_2)(Q - \bar{Q}) + \left(1 + \frac{n_{eff}^2}{n_{cl}^2}\right)\frac{n_{cl}^2}{n_{co}^2 u_2^2} im(\zeta_0)(R - \bar{R}) - \left(1 + \frac{n_{eff}^2}{n_{cl}^2}\right)\left[\frac{n_{cl}^2 im(\zeta_0)}{n_{co}^2 u_2}F_2 + \frac{1}{u_1}im(G_2)\right] \times (S - \bar{S}) + \frac{2n_{eff}}{u_2}\left(\frac{Z_0\zeta_0}{n_{co}^2}G_2 - \frac{1}{Z_0}F_2\right)(S + \bar{S})\right\} \tag{23}$$

$$P_2 = \left(E_{1m}^{cl}\right)^2 P_{2,coeff} \quad (24)$$

$$P_{3,coeff} = \frac{\pi^3 a_{co}^2 a_{cl}^2 u_1^4 u_2^4 J_1^2(u_1 a_{co})}{16 w_3^2 K_1^2(w_3 a_{cl})} \times \left\{\left[\frac{n_{eff} Z_0}{n_{surr}^2} G_3^2 - \frac{n_{eff}}{Z_0} F_3^2 - \left(1 + \frac{n_{eff}^2}{n_{surr}^2}\right) F_3 im(G_3)\right] \times [K_2^2(w_3 a_{cl}) - K_1(w_3 a_{cl}) K_3(w_3 a_{cl})] + \left[\frac{n_{eff} Z_0}{n_{surr}^2} G_3^2 - \frac{n_{eff}}{Z_0} F_3^2 + \left(1 + \frac{n_{eff}^2}{n_{surr}^2}\right) F_3 im(G_3)\right] \times [K_0^2(w_3 a_{cl}) - K_1^2(w_3 a_{cl})]\right\} \quad (25)$$

$$P_3 = \left(E_{1m}^{cl}\right)^2 P_{3,coeff} \quad (26)$$

Adding equations (28), (30) and (32), we get:

$$P_1 + P_2 + P_3 = \left(E_{1m}^{cl}\right)^2 \left[P_{1,coeff} + P_{2,coeff} + P_{3,coeff}\right] \quad (27)$$

Total Power is equal to 1 watt as given in Equation (20), soby substituting this calculated result in equation (27) we can write the Equation as:

$$E_{1m}^{cl} = \sqrt{\frac{1}{P_{1,coeff} + P_{2,coeff} + P_{3,coeff}}} \quad (28)$$

The various unknown quantities used in power calculations coefficients ($P_{1,coeff}$, $P_{2,coeff}$& $P_{3,coeff}$) are expressed below:$Q =$

$$\theta_J N_1^2(u_2 a_{co}) + \theta_N J_1^2(u_2 a_{co}) - 2\theta_{JN} J_1(u_2 a_{co}) N_1(u_2 a_{co}) \quad (29)$$

$$\overline{Q} = \overline{\theta_J} N_1^2(u_2 a_{co}) + \overline{\theta_N} J_1^2(u_2 a_{co}) - 2\overline{\theta_{JN}} J_1(u_2 a_{co}) N_1(u_2 a_{co}) \quad (30)$$

$$R = \frac{1}{4}\theta_J [N_2(u_2 a_{co}) - N_0(u_2 a_{co})]^2 + \frac{1}{4}\theta_N [J_2(u_2 a_{co}) - J_0(u_2 a_{co})]^2 - \frac{1}{2}\theta_{JN} [N_2(u_2 a_{co}) - N_0(u_2 a_{co})] \times [J_2(u_2 a_{co}) - J_0(u_2 a_{co})] \quad (31)$$

$$\overline{R} = \frac{1}{4}\overline{\theta_J} [N_2(u_2 a_{co}) - N_0(u_2 a_{co})]^2 + \frac{1}{4}\overline{\theta_N} [J_2(u_2 a_{co}) - J_0(u_2 a_{co})]^2 - \frac{1}{2}\overline{\theta_{JN}} [N_2(u_2 a_{co}) - N_0(u_2 a_{co})] \times [J_2(u_2 a_{co}) - J_0(u_2 a_{co})] \quad (32)$$

$$S = \frac{1}{2}\theta_J N_1(u_2 a_{co})[N_0(u_2 a_{co}) - N_0(u_2 a_{co})] + \frac{1}{2}\theta_N J_1(u_2 a_{co})[J_0(u_2 a_{co}) - J_2(u_2 a_{co})] - \frac{1}{2}\theta_{JN}\{N_1(u_2 a_{co})[J_0(u_2 a_{co}) - J_2(u_2 a_{co})] + J_1(u_2 a_{co})[N_0(u_2 a_{co}) - N_2(u_2 a_{co})]\} \quad (33)$$

$$\overline{S} = \frac{1}{2}\overline{\theta_J} N_1(u_2 a_{co})[N_0(u_2 a_{co}) - N_0(u_2 a_{co})] + \frac{1}{2}\overline{\theta_N} J_1(u_2 a_{co})[J_0(u_2 a_{co}) - J_2(u_2 a_{co})] - \frac{1}{2}\overline{\theta_{JN}}\{N_1(u_2 a_{co})[J_0(u_2 a_{co}) - J_2(u_2 a_{co})] + J_1(u_2 a_{co})[N_0(u_2 a_{co}) - N_2(u_2 a_{co})]\} \quad (34)$$

$$\theta_J = a_{cl}^2[J_2^2(u_2 a_{cl}) - J_1(u_2 a_{cl}) J_3(u_2 a_{cl})] - a_{co}^2[J_2^2(u_2 a_{co}) - J_1(u_2 a_{co}) J_3(u_2 a_{co})] \quad (35)$$

$$\theta_N = a_{cl}^2[N_2^2(u_2 a_{cl}) - N_1(u_2 a_{cl}) N_3(u_2 a_{cl})] - a_{co}^2[N_2^2(u_2 a_{co}) - N_1(u_2 a_{co}) N_3(u_2 a_{co})] \quad (36)$$

$$\theta_{JN} = a_{cl}^2\left\{J_2(u_2 a_{cl}) N_2(u_2 a_{cl}) - \frac{1}{2}[J_1(u_2 a_{cl}) N_3(u_2 a_{cl})] + [J_3(u_2 a_{cl}) N_1(u_2 a_{cl})]\right\} - a_{co}^2\left\{J_2(u_2 a_{co}) N_2(u_2 a_{co}) - \frac{1}{2}[J_1(u_2 a_{co}) N_3(u_2 a_{co})] + [J_3(u_2 a_{co}) N_1(u_2 a_{co})]\right\} \quad (37)$$

$$\overline{\theta_J} = a_{cl}^2[J_2^2(u_2 a_{cl}) + J_1^2(u_2 a_{cl})] - a_{co}^2[J_2^2(u_2 a_{co}) + J_1^2(u_2 a_{co})] \quad (38)$$

$$\overline{\theta_N} = a_{cl}^2[N_2^2(u_2 a_{cl}) + N_1^2(u_2 a_{cl})] - a_{co}^2[N_2^2(u_2 a_{co}) + N_1^2(u_2 a_{co})] \quad (39)$$

$$\overline{\theta_{JN}} = a_{cl}^2[J_0(u_2 a_{cl}) N_0(u_2 a_{cl}) + J_1(u_2 a_{cl}) N_1(u_2 a_{cl})] - a_{co}^2\{J_0(u_2 a_{co}) N_0(u_2 a_{co}) + J_1(u_2 a_{co}) N_1(u_2 a_{co})\} \quad (40)$$

When the coupling coefficients have been resolved to portray the exchange of optical power from the core mode to each of the possible cladding mode designs, the LPFG's transmission range can be straightforwardly obtained.

VI. Simulation Results of Transmission Spectrum

There are a few unique strategies for computing transmission range, for example, fundamental strategy, Transfer matrix method and Equation method. The point by point correlations between these strategies are given in [11]. In the precision, multifaceted nature of each technique is simulated and obtained. In this paper we pick necessary technique as it give the definite solution of the transmission range.

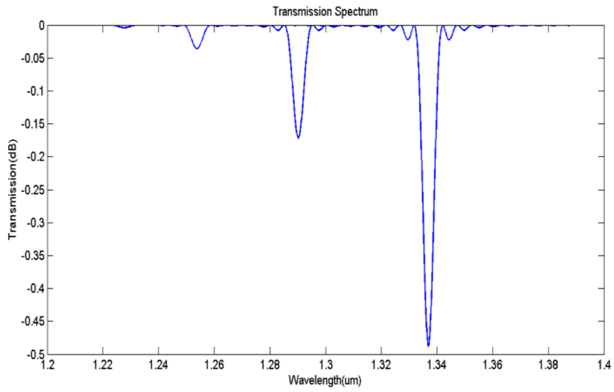

Fig. 4. Simulated Transmission Spectrum for LPFG.

VII. Simulation Results of Transmission Spectrum

In this paper we have hypothetically demonstrated Long Period Fiber Grating (LPFG) using Triple layer geometry. Moreover, discussion is made about the deficiencies of modelling employed using Two-Layer geometry. Finally, simulation results and numerical analysis is performed and found that Triple-Layer geometry is the most refreshed, exact strategy for hypothetically modelling Long Period Fiber Gratingat the expense of increased numerical complexity nature when contrasted with demonstrating utilizing two-layer geometry.

References

[1] A. M. Vengsarkar, P. J. Lemaire, J. B. Judkins, V. Bhatia, T. Erdogan, and J. E. Sipe, Long-Period Fiber Gratings as Band-Rejection Filters, Journal of Lightwave Technology, vol. 14, pp. 58-65, 1996.

[2] V. Bhatia, Applications of long-period gratings to single and multi-parameter sensing, Optics Express 4(11), pp. 457-466, 1999.

[3] A. Singh, S. B. Rana, M. Singh, A. Sharma, Study and investigation of long period grating as refractive index sensor, Optik, vol 125, No 7, pp.1860–1863, 2014.

[4] K.R. Cooper, J. Elster, M. Jones, R.G. Kelly, Optical fiber-based corrosion sensor systems for health monitoring of aging aircraft, IEEE Systems Readiness Technology Conference, pp. 847-856, 2001.

[5] J. A. Besley, T. Wang, L. Reekie, Fiber Cladding Mode Sensitivity Characterization for Long-Period Gratings, Journal of Lightwave Technology, 21 (3), pp. 848 - 853, 2003.

[6] A. Singh, D. Engles, A. Sharma, M. Singh, Temperature sensitivity of long period fiber grating in SMF - 28 fiber, Optik, Vol 125, No 1, pp.457–4601, 2014.

[7] Erdogan, T. Cladding-mode resonances in short- and long-period fiber grating filters. Journal of the Optical Society of America A 14(8): pp.1760-1773, 1997.

[8] J.A Buck, Fundamentals of Optical Fibers, John Wiley and Son Inc, New York, 1995.

[9] W. V Etten & J. V. D Plaats, Fundamentals of optical fiber communications. New York: Prentice Hall (1991).

[10] T.Erdogan, Fiber grating spectra, Journal of Lightwave Technology 15(8):1277-1294, 1997.

[11] Y. Yang, Z. Gu, Comparing and analysis of calculation methods of long period fiber gratings transmission spectra, Optik, 124, pp. 2234– 2240, 2013.

